‘Wolf rahm’: archaeological evidence for the veracity of an old term

Tim Young and Sean Taylor

ABSTRACT: The medieval tin smelting site at Brownie Cross, Devon, lies just 4km from the tungsten deposit of Hemerdon Ball and smelted alluvial ores commonly contaminated by wolframite. The slag is present as fragments of thin sheets, probably scraped from the surface of the tin in the float, the bases of which bear inclusions of tungsten metal, tin oxides, wolframite and hard head. The low-tungsten slags variously comprise spinels, ilmenite, olivine and Fe-cordierite in glass. The high-tungsten slags are glass with an unusual Fe-Mn-Mg tungstate (tungstate A) and commonly show relict emulsion textures, in which the tungsten-rich component shows extreme enrichment of tin with respect to silica. The ability of the tungsten-rich slags to capture tin demontrates the problems faced by medieval smelters in Germany, who named the contaminant ‘Wolf rahm’ (wolf’s spit, foam, froth or dross), implying that the slag devoured tin, like a wolf devouring lambs.

Introduction

The co-occurrence of tin and tungsten mineralization is a well-known geological phenomenon (see Alderton 1993 for a discussion of Sn-W mineralisation in SW England), occurring in Europe in association with the late Variscan granites of Portugal, the French Massif Central, SW England and the Erzgebirge (the boundary of Germany with the Czech Republic). The Erzgebirge region was the home of Georg Pawer (Georgius Agricola; 1494-1555) who provides us with the earliest recorded usage of the term *lupi spuma* (Bandy and Bandy 1955; translated as wolf’s spit, froth or foam). It is assumed that this Latin expression was a translation of the equivalent expression in German, *Wolf rahm*, not documented directly until 200 years later in the works of Henckel (1725) and Wallerius (1747), for the mineral now known as wolframite ($(Fe,Mn)WO_4$). It is generally accepted that ‘wolf’s froth’ refers to the drastic loss of tin to the slag (froth) during smelting when the ore is contaminated by wolframite (‘It tears away the tin and devours it like a wolf devours a sheep’ Sisco and Smith 1951). The issue of contamination was problematic because of the similarity in density of cassiterite (~7 g/cm^3) and wolframite (7-7.5 g/cm^3), making them difficult to separate through the normal process of vanning. Pryce (1778) described the problem in Cornwall:

> ‘Our Gossan Lodes often produce Tin at a shallow level in tolerable plenty; and chiefly that Gossan which is of the most ferruginous stamina, and we believe from then denominated Gal, which is old Cornish British, and signifies rust; and being really an inferior Iron Ore, answers in name to its appearance. The Germans call it Wolffram, and define it as a kind of Manganese. In this kind of Gossan, after the Tin is separated from all other impurities by repeated ablutions, there remains a quantity of this mineral substance, Gal; which being of equal gravity, cannot be separated from the Tin Ore by water; therefore it impoverishes the Metal, and reduces its value down to eight or nine parts for twenty of Mineral, which without this brood, so called, might fetch twelve for twenty.’

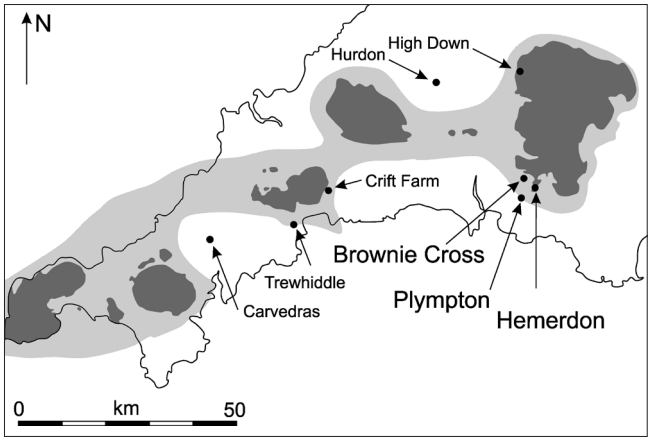

Figure 1: Location map showing location of main places mentioned in the text. The light tone indicates the sub-surface extent of the Cornubian batholith; the dark tone indicates where granite crops out at the surface. Geology after Dines 1956 and Alderton 1993.

Scheele (1781) investigated a mineral known in Swedish as 'tungsten' (literally 'heavy stone'; now known as scheelite, $CaWO_4$) and showed it was a calcium salt of a new acid, tungstic acid. It was realised this acid was the oxide of an unknown element – which was initially proposed to be named scheelium, but tungsten soon gained preference. In 1783 Juan José de Elhuyar y de Zubice and his brother, Fausto, analysed wolframite and demonstrated it contained the same new oxide as tungsten (Luyart and Luyart 1783). They produced the metal by reduction of the oxide with charcoal and named it volfram. The name tungsten had been used previously, but only in a theoretical sense, because the element had not been isolated before the Elhuyar brothers' work. Modern formal usage continues the confusion, with tungsten now being the accepted element name, although W is used for its symbol.

In SW England the most important example of tungsten mineralisation (occurring together with tin) is the Hemerdon Ball (or Bal) deposit, on the SW side of Dartmoor about 4km NE of Plympton. The mineralisation has been described by Dines (1956), Bray and Spooner (1983) and Alderton (1993). The Hemerdon deposit is currently the fourth largest tungsten resource known in the world and the largest in the western hemisphere.

The medieval tin smelting site at Brownie Cross, Shaugh Prior, Devon (Taylor *et al* 2014) lies 4km NW of Hemerdon Ball (Fig 1). It was discovered and excavated by Historic Environment Projects, Cornwall Council, which had been commissioned by South West Water to undertake a programme of archaeological investigations along the route of the 13.5km-long Avon Water Main Renewal Project in April and May 2009. The remains included evidence for two structures: Structure 1 comprised the remains of the smelting furnace and associated features (including a mouldstone) and Structure 2 was a shelter or store. Radiocarbon dates indicate activity within the late 13th or early 14th centuries. The site lies on a ridge-top and there is little indication that the site could have employed water power. It is accordingly interpreted as having been blown manually, but other aspects of the technology and residues appear similar to those of the later blowing houses. The potential of the residues to provide information on an important period of evolution of tin smelting technology was identified in the assessment of the residues (Young and Kearns 2011) and a thorough analytical investigation was commissioned (Young 2011). This investigation demonstrated that the residues had an unusual tungsten-rich composition. It is the potential of these residues to shed light on the origin of the term wolf rahm that is the subject of this paper; the reader is referred to the article by Taylor *et al* (2014) for a full report on the site and its implications for the evolution of medieval tin smelting.

Methods

Seventeen of twenty samples (Table 1) drawn from the assessed materials were analysed. The samples were from two contexts (1146) and (1349B), each with a large slag assemblage, to permit determination of the variety within the two assemblages. Both contexts were slag deposits lying over the area of pit 1398 in the SW part of Structure 1 (Taylor *et al* 2014, 200-213).

Electron microscopy was undertaken on the Cambridge Instruments (LEO) S360 analytical electron microscope in the School of Earth and Ocean Sciences, Cardiff University. Microanalysis was undertaken using the system's Oxford Instruments INCA ENERGY energy-dispersive X-ray analysis system (EDS). All petrographic images presented in this report are backscattered electron photomicrographs. The polished blocks for investigation on the SEM were prepared in the Earth Science Department, The Open University. X-ray diffraction was undertaken on the Philips PW1710 automated powder diffractometer, also in the School of Earth and Ocean Sciences, Cardiff University.

In order to make the microanalytical results comparable across materials (and also sites), no attempt has been made to adjust for the oxidation state of elements with variable valency. The figures have therefore been constructed with elements expressed as oxides in weight% calculated stoichiometrically, except for mineral structure calculations, where the measured

Table 1. Average bulk composition of each sample. Microanalysis by EDS, expressed in normalised wt% with oxygen calculated stoichiometrically.

	context	n	Na_2O	MgO	Al_2O_3	SiO_2	P_2O_5	S	K_2O	CaO	TiO_2	V_2O_5	CrO_3	MnO	FeO	ZrO_2	SnO	WO_3
Group 1																		
AVN6	1349B	2	1.47	3.69	17.27	46.41	0.66	0.00	0.77	1.15	3.59	0.00	0.00	0.81	11.35	0.00	12.83	0.00
Group 2																		
AVN1	1349B	3	0.95	2.49	13.19	31.63	0.54	0.00	1.11	0.69	2.85	0.00	0.00	0.69	17.29	0.00	21.77	6.79
AVN2	1349B	10	0.76	1.43	11.44	24.93	0.11	0.00	1.09	1.46	6.88	0.05	0.00	1.45	13.32	1.27	25.25	10.56
AVN5	1349B	6	0.89	2.32	11.01	28.63	0.54	0.00	1.00	0.55	2.94	0.00	0.00	0.71	17.62	0.00	25.65	8.15
Group 3																		
AVN4	1349B	3	0.26	0.46	4.17	10.88	0.36	0.00	0.38	0.00	0.62	0.00	0.00	3.05	14.33	0.00	24.72	40.78
AVN7	1349B	5	0.69	1.42	9.31	23.40	0.38	0.00	0.89	0.81	1.92	0.00	0.00	1.68	17.89	0.14	21.59	19.87
AVN8	1349B	2	0.00	0.74	5.21	16.20	0.55	0.00	0.13	0.67	0.73	0.00	0.00	2.59	15.90	0.00	24.56	32.73
AVN9	1146	2	0.58	1.36	7.54	21.31	0.49	0.00	0.20	0.57	1.40	0.00	0.00	2.18	14.51	0.00	20.28	29.59
AVN10	1146	9	0.50	1.12	6.61	18.34	0.46	0.00	0.63	0.56	1.14	0.00	0.00	2.40	14.91	0.09	18.99	34.24
AVN12	1146	10	0.62	1.58	8.31	21.92	0.30	0.00	0.58	0.63	1.79	0.00	0.00	2.25	14.89	0.32	18.66	28.16
AVN13	1146	9	0.47	1.13	6.47	17.97	0.33	0.00	0.47	0.47	1.11	0.00	0.00	2.30	14.13	0.19	21.52	33.34
AVN15	1146	5	0.47	1.26	7.58	18.70	0.28	0.00	0.30	0.64	1.30	0.00	0.00	2.36	15.38	0.19	18.67	32.87
AVN16	1146	3	0.42	1.29	6.86	19.28	0.15	0.00	0.48	0.58	1.15	0.00	0.00	2.40	14.78	0.29	19.74	32.57
AVN17	1146	3	0.37	1.29	6.77	18.32	0.17	0.00	0.45	0.57	1.42	0.00	0.00	2.44	14.50	0.26	20.78	32.67
AVN18	1146	2	0.46	1.46	7.34	20.29	0.45	0.00	0.28	0.50	1.42	0.00	0.00	2.33	15.14	0.00	18.16	32.18
AVN19	1146	3	0.55	1.27	6.78	18.91	0.36	0.00	0.48	0.49	1.27	0.00	0.00	2.37	15.22	0.34	19.37	32.61
AVN20	1146	4	0.40	1.56	8.23	21.55	0.39	0.36	0.00	0.52	1.62	0.00	0.00	2.32	14.76	0.00	17.51	30.78

oxygen has been used. Iron is expressed as FeO, manganese as MnO, tin as SnO and tungsten as WO_3. Sulphur is present mainly in sulphides, so has been presented as S in the data.

Throughout this report standard mineral terminology is applied to both natural and anthropogenic materials – although artificial phases are no longer strictly considered to be minerals. A detailed description of the slag mineralogy is provided in the Appendix.

Slag composition

Three distinct groups of slags were identified, based on their composition (Table 1; Fig 2) and microstructure (Fig 3):

Group 1 slag (sample AVN6; Fig 3a) has bulk tungsten contents below detection; the sample was a simple glass (at least at the limits of the resolution of the SEM) with some flow-banding bearing small prills of tin. The bulk composition (Table 1) includes a high concentration of silicon and aluminium, and moderately high levels of iron, sodium, magnesium, calcium, titanium and tin. This composition is similar to slags previously recorded from the medieval smelting site at Crift Farm, Cornwall (Malham *et al* 2002).

Group 2 slags (samples AVN1, 2, 5; Fig 3b) have 5-15% WO_3 and FeO/WO_3 of > 1; the material is

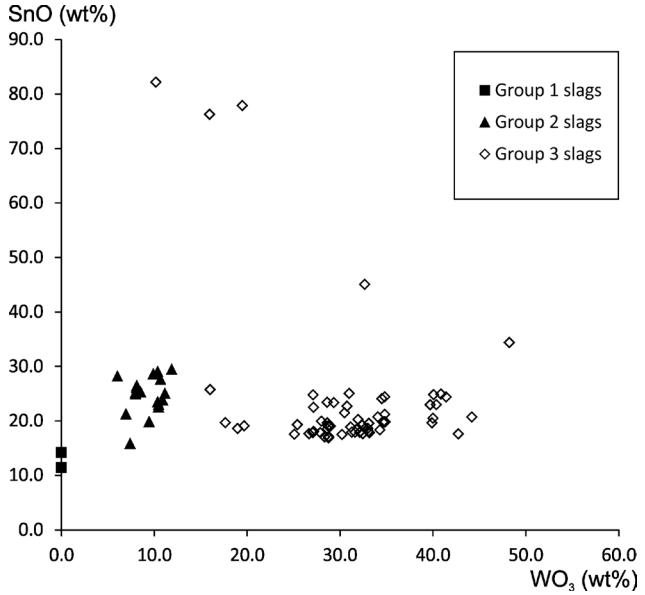

Figure 2: Plot of SnO vs WO_3 for area EDS analyses of slag samples. Points are analyses of individual areas.

dominantly glass, which locally bears minor olivine, spinels, scheelite and ilmenite. One sample (AVN5) shows small hammerscale-like particles of iron and tin oxides, overgrown by olivine and tungstate A. Sample AVN1 bears inclusions of tungsten metal (aggregates of blebs of up to about 5µm, overgrown by a neoform tungstate of wolframitic composition) near one margin. These 'exotic' inclusions are discussed in more detail below. Group 2 slags have lower aluminium and silicon contents than Group 1, although still higher than Group 3. They typically show a slightly higher alumina to silica

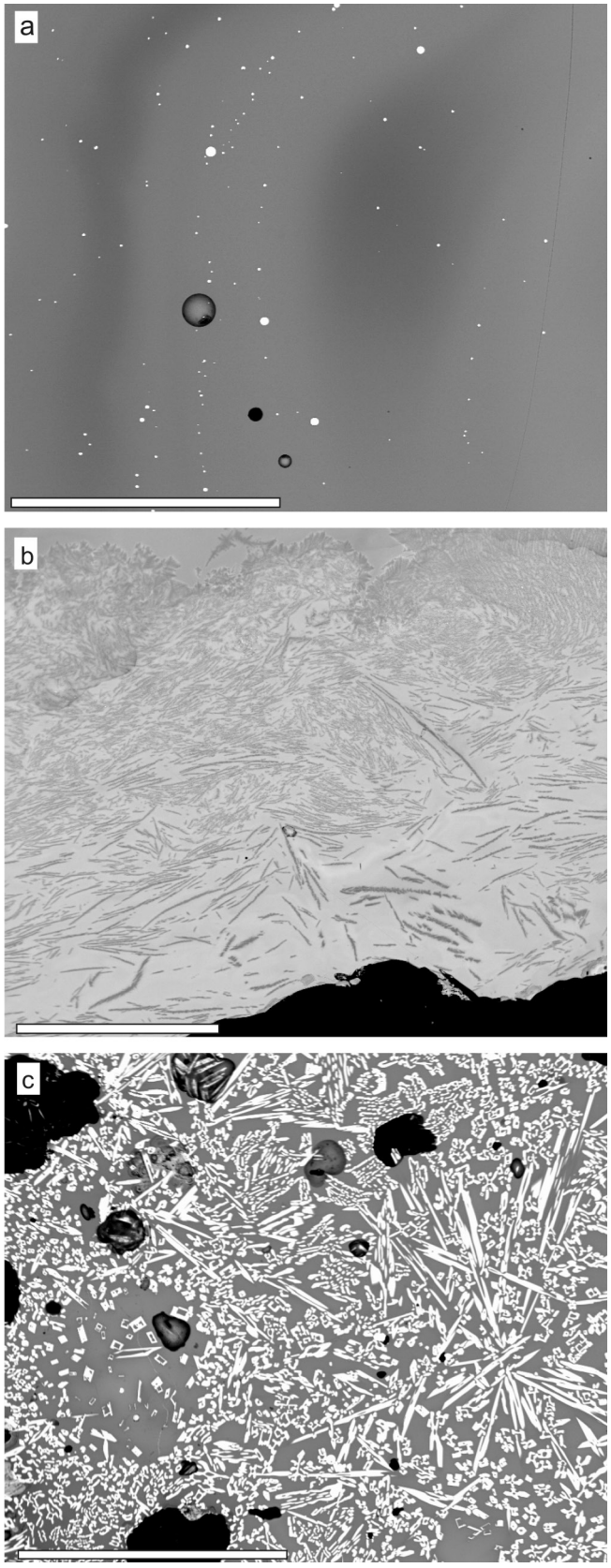

Figure 3: BSEM images of samples showing representative slag textures. a) Group 1 slag (AVN6), glass of variable composition with abundant tin prills (bright spots). b) Group 2 slag (AVN2), slag with marginal crystallisation of dendrites of ilmenite and spinels. The interior is glassy or microcrystalline. c) Group 3 slag (AVN8), slag with prismatic crystals of tungstate A in glass (scale bars all 500µm).

ratio than the group 3 slags although the fields overlap (the average alumina:silica ratio for Group 2 is 0.42, whereas for Group 3 it is 0.37). The Group 2 slags are also distinguished by elevated titanium (average of 4.1% TiO_2, compared with an average of 3.5% in Group 1 and 1.3% in Group 3) and iron contents. These two features suggest that Fe-Ti oxides may have been a significant component of the furnace feed. The content of tin is approximately double that of Group 1, with 22-26% SnO.

Group 3 slags (samples AVN 4, 8, 9, 10, 12, 13, 15, 16, 17, 18, 19 and 20; sample AVN7 is transitional to Group 2; Fig 3c) have >15% WO_3 and FeO/WO_3 < 1; the principle crystalline phase is tungstate A (see below). This mineral occurs in elongate crystals, in some samples with variations in their width demarcating the former locations of blebs within an emulsion (a mixture of two mutually immiscible liquids suspended in each other). The proportion of glass in this group is typically lower than in the other groups. These samples commonly contain inclusions of tin oxides, wolframite, hardhead (tin-iron intermetallics) and tungsten, discussed in more detail below. The chemical composition shows low concentrations of silica and alumina (less than half that in Group 1). As well as the strongly elevated concentration of tungsten, both iron and manganese are also present in large proportion, reflecting the composition of the wolframite in the ore. In contrast calcium is relatively depleted, demonstrating that the ore was not rich in scheelite.

The three compositional groups of slags represent three distinct source materials. Group 1 slags were the result of smelting a relatively pure cassiterite concentrate, Group 2 from smelting ores in which both Fe-Ti oxides and wolframite were contaminants (the slightly more aluminous slag composition hints that kaolinite may have been a contaminant too) and Group 3 slags resulted from the smelting of ores heavily contaminated with wolframite. These bear a general similarity to the slags from the 19th century shaft furnace at Schlaggenwald, Bohemia, where similar tungsten contamination occurred (Louis 1911, 38).

Evidence for emulsions

Five of the Group 3 slag samples show textural evidence for crystallisation from an emulsion (Fig 4). Two samples (AVN10 and 18) show this to a small degree, but in three samples (AVN13, 16 and19) the emulsion forms a very prominent feature. The relicts of the emulsions are marked not only by a variation in the size and

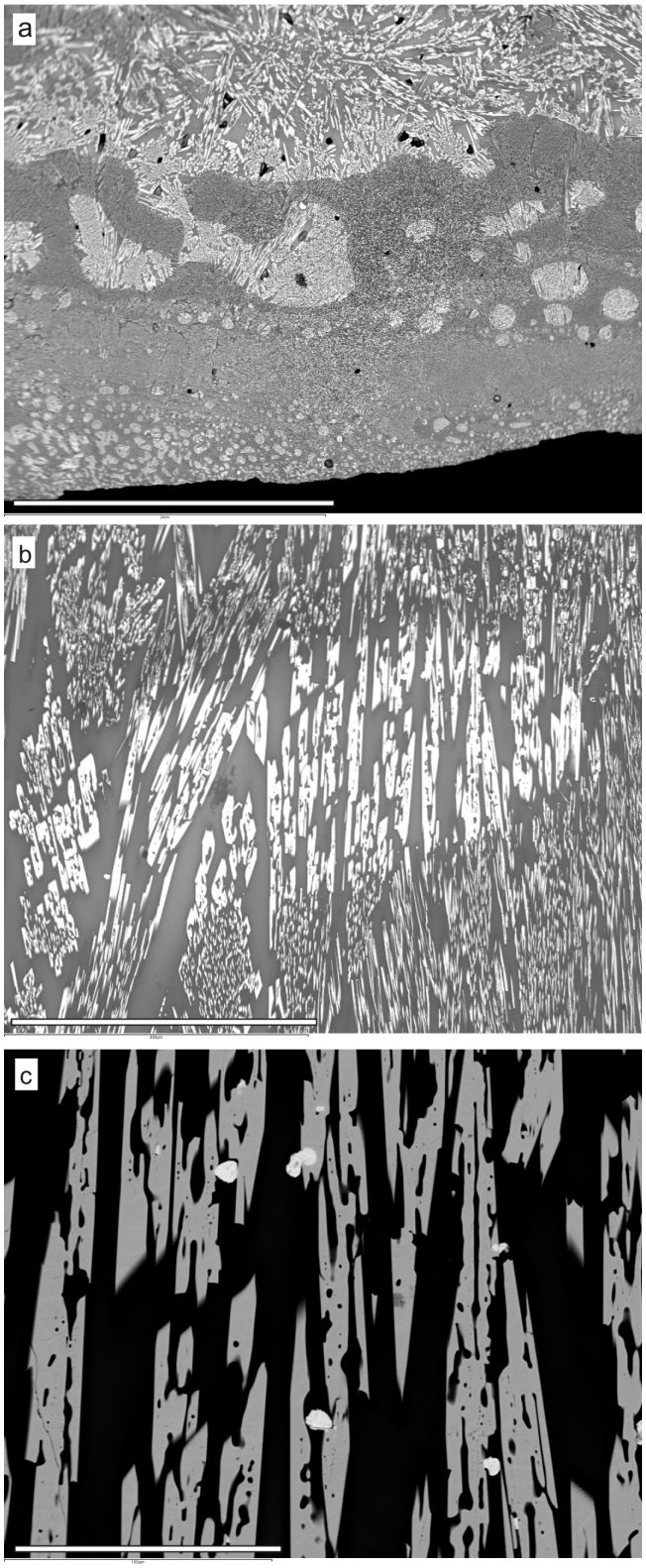

Figure 4: BSE micrographs showing microstructural evidence for slag emulsions. a) Complex emulsion relationships, including a major boundary just above the centre with irregularities that resemble density-driven boundary deformation (loading). AVN13 (scale bar 2mm). b) Typical preservation of a tungsten-rich emulsion droplet; the tungstate A crystals cut across the bleb, but thicken markedly in the tungsten-rich zone. AVN18 (scale bar 400µm). c) Detail of the bleb in b) showing tin droplets (white) trapped by the tungstate crystals (pale grey). AVN18 (scale bar 100µm).

continuity of the crystals of tungstate A as they traverse the compositional elements, but also by variation in the composition of the glass that forms the matrix. For AVN18, the interstitial glass composition in the zone of denser tungstate crystals (centre of Fig 4b) includes 11% tungsten, 35% tin and 11% silicon, whereas the glass immediately outside this zone contains 4% tungsten, 26% tin and 29% silicon. Figure 4c also illustrates the frequent occurrence of small tin prills (up to 10µm diameter) in the tungsten-rich zones but they are relative rare in the tungsten-poor areas.

Bulk microanalysis of the materials involved in these textures shows a tungsten-poor component with 26-32% WO_3 and a tungsten-rich component with 33-47% WO_3. As was noted for the pattern of bulk slag compositions, the ratio of tin and tungsten oxides to silica is markedly elevated in the tungsten-rich blebs. The tungsten-poor components of the emulsions have $SnO:SiO_2$ of 0.74-1.09 (mean 0.91), whereas the tungsten-rich components have $SnO:SiO_2$ of 0.76-2.35 (with an outlier at 4.55; mean 1.80). The variability and overlap of compositions of the components suggests that these emulsions were not due to two distinct, particular inputs, but simply poor mixing of a variable input.

Inclusions within the slags

There are also inclusions and zones within the slag samples that appeared to be distinct from the bulk of the silicate slag. These materials include a variety of rather poorly characterised tin oxides (including examples from AVN7, 10, 15, 17, 19 and 20), metallic tungsten (AVN1, 10, 17, 19 and 20), coarse grains of wolframite (AVN12, 15 and 17), unusually coarse grains of tungstate A (AVN19 and 20) and examples of the iron-tin intermetallics, FeSn and $FeSn_2$, known as hardhead (AVN10 and 20). These materials are all interpreted as inclusions carried by, or associated with, the slag, but of quite distinct origin. Many of these inclusions rest near or on the margins of the slag (probably particularly the basal surface) suggesting that they may have been acquired from the slag-metal or slag-dross interface.

Tin oxides are a major component of these materials but have proved difficult to analyse satisfactorily; their precise nature remains uncertain. For many of the EDS analyses the measured oxygen content is in excess of what would be required for the minerals in the normal oxidation regime for tin: romarchite, hydroromarchite and cassiterite (Dunkle *et al* 2003). There is a particular problem in generating good analyses of light elements by EDS when they occur with an element as heavy as

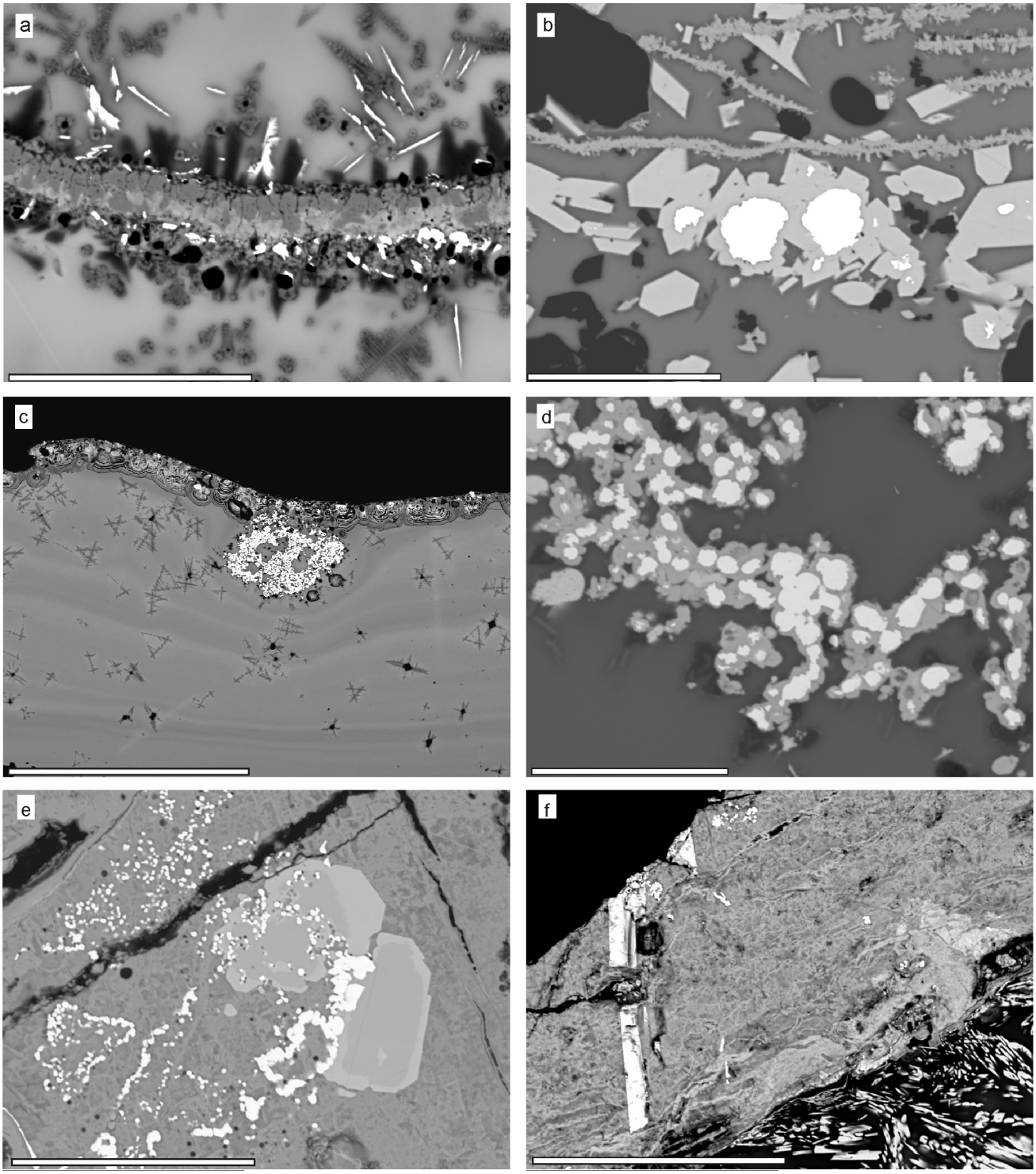

Figure 5: BSE micrographs of slags with particulate impurities derived from the tin. a) Hammerscale-like particle of iron and tin oxides, supporting olivine and spinel minerals in the slag. The lower part of the scale is tin-rich (pale grey), the upper part close to end-member magnetite (mid grey). This is interpreted as an oxide scale formed on the surface of liquid iron-bearing tin and subsequently incorporated into the slag. The lower face shows numerous tin blebs (white) associated with the tin oxide. AVN5 (scale bar 50μm). b) Coarse-grained area on the margin of a normal tungsten-rich slag. The marginal zone includes blebs of tungsten (white) overgrown (and replaced?) by tungstate (pale grey). Close to the tungsten this seems close to a simple tungsten oxide, but the outer parts of the euhedral crystals show the normal Mn-, Mg- and Fe- substitution of tungstate A. These tungstate grains have formed the substrate for the growth of some minor olivine. The upper part of the image shows plate-like growths of a tin oxide, possibly another type of 'scale'. AVN17 (scale bar 30μm). c) An inclusion rich in metallic tungsten (light) on the margin of a glassy slag. The devitrified margin contains abundant tin blebs (bright spots), so is probably the original tin-contact. AVN1 (scale bar 600μm). d) Detail of the inclusion in c). The metallic tungsten (bright) is coated in a thin layer of tungstate and traps a few prills of tin (most now oxidised). AVN1 (scale bar 30μm). e) Detail within the complex oxide zone in AVN20. Euhedral hardhead (FeSn inside $FeSn_2$; light grey with a slightly darker core associated with strings of tungsten inclusions (white) marking the polygonal outlines of prior grains in a tin oxide matrix. AVN19 (scale bar 60μm). f) Elongate hardhead crystals and minor isolated blebs of tungsten within a tin oxide matrix. AVN10 (scale bar 90μm).

tin; small analytical errors are magnified into large formula errors. These oxide phases often provide a matrix, frequently extending as a thin layer along the base of the slag sheet, within which hardhead and tungsten occur (*eg* Fig 5e, 5f), so it would be very useful to be certain whether these materials represent a high temperature oxidation of tin or a low temperature alteration, but that is not possible on the current evidence. It is significant however, that in these major zones of tin oxides there were no occurrences of tin as metal, suggesting an origin from the primary high temperature oxidation of the underlying surface, rather than an in-situ secondary alteration of tin inclusions.

Another oxide material is evidenced by a laminar inclusion, 20-25µm thick and 2mm long, present in AVN5 (Fig 5a), which strongly resembles flake hammerscale. It is formed of two oxide layers. The outer (?) layer is dense, columnar and, at least in its outermost part, close to end-member magnetite. The inner (?) porous layer is a mixed iron-tin oxide of uncertain nature with trapped blebs of tin. Both sides of the scale were overgrown by an olivine ($Fa_{70-72}Fo_{30-28}$ with 2% Mn substitution; 10µm long) and by blades of tungstate A (10µm long). Laminar particles are also present near the base of the slag sheet in AVN17, but these are solely of tin oxide.

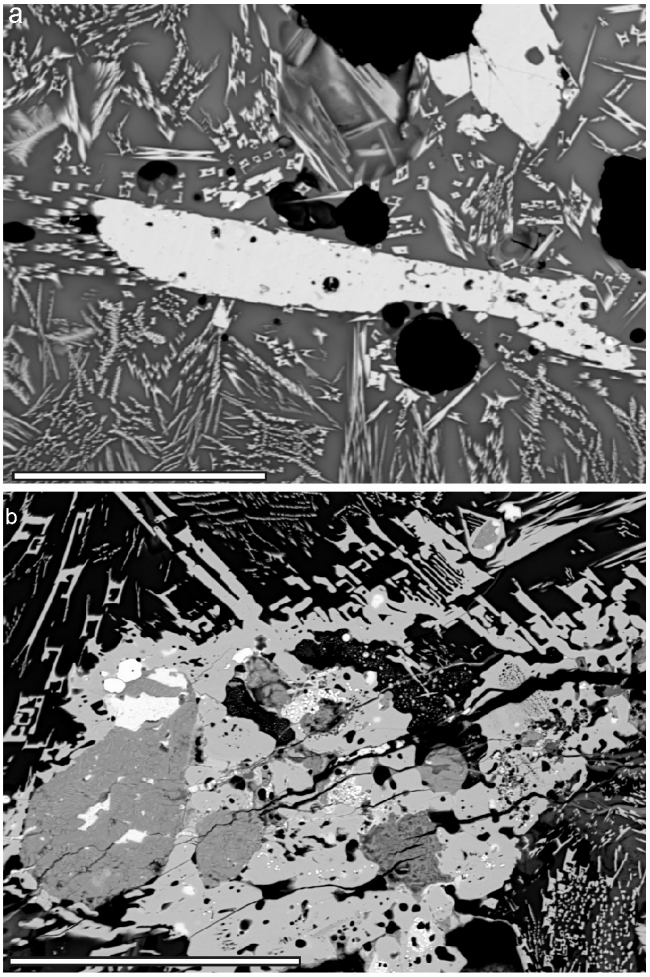

Figure 6: BSE micrographs of coarse-grained tungstates.a) a relict grain of wolframite with very thin tungstate A overgrowths (centre, white) in a slag with abundant crystals of neoform tungstate A. It is approximately 70% ferberite and 30% hueberneite over most of the section, but changes towards 32% ferberite and 68% huebnerite near the lower margin. Sample AVN12. Scale bar 100µm. b). coarse neoform tungstate A, showing inclusions of tin and tin oxides (white).

Metallic tungsten occurs in several samples in the form of small rounded blebs (often rather irregular where they are overgrown by tungstate minerals). In AVN1 (Fig 5c, 8d) the blebs are typically up to about 5µm and overgrown with a thin ferberitic skin forming an aggregate particle, also associated with, or trapping, similarly sized tin prills. In AVN10 (Fig 5f) and AVN20 (Fig 5e) the tungsten blebs are much smaller, are contained within a matrix of tin oxide, and are spatially associated with hardhead. Slightly larger tungsten particles occur in AVN17 (Fig 5b) and these are overgrown by tungstate A in euhedral grains.

Euhedral hardhead was recorded in two samples. In both cases it was present within a matrix of tin oxides and was closely associated with small particles of metallic tungsten. In AVN10 (Fig 5f) the basal layer of the slag sheet contained elongate crystals of FeSn of at least 80µm by 10µm while those in AVN20 were more equant grains up to 50µm (Fig 5e), with cores of FeSn surrounded by $FeSn_2$.

A few samples show large crystals of wolframite, typically close to the iron end-member (ferberite, $FeWO_4$) but locally with margins increasingly rich in the manganese end-member (huebnerite, $MnWO_4$). These are interpreted as natural grains inherited from the furnace feed, locally with overgrowths of tungstate A formed in the slag (Fig 6a).

One interesting component of the inclusions in AVN19 and AVN20 is the presence of very large crystals (equant grains of up to 300µm) of tungstate A with rounded outlines and carious textures indicative of resorption (Fig 6b). The crystals are typically near to tin/tin oxides. Their size compared with the tungstate mineral in the adjacent slag matrix suggests that these crystals have been inherited from an earlier slower phase of crystallisation, perhaps within the furnace.

Variation in bulk composition

The slag analyses help shed light on the smelting process with varying degrees of tungsten-contamination. Figure

2 shows the variation of tin with tungsten for the bulk sample analyses. The proportion of tin in the Group 2 slags is higher than in the Group 3 slags, but both have a higher proportion of tin than the Group 1 slag. This, however, does not take into account the diluting effect of the tungsten on the other slag components; it passes from the ore, through the smelting process and into the slag. The present data are not sufficient for the construction of a mass-balance description of the smelting, but one approach to improve understanding of the take-up of tin and tungsten by the slag is to normalise the data against the proportion of silica and alumina. These elements will have entered the smelt as contaminants of the ore and from degradation of the furnace structure. They may represent the closest to a 'constant' that can be found, in order to determine the tin-tungsten relationship.

Figure 7 shows an irregular distribution of data but a clear increase in the amount of tin contained in the slag, compared to the amount of silica and alumina, with increasing tungsten content. This graph can be considered as showing the relative loss of tin to a slag formed from a fixed amount of silica and alumina. Thus, for a volume of tungsten-free slag containing 1kg of silica and alumina, there will be just under 200g

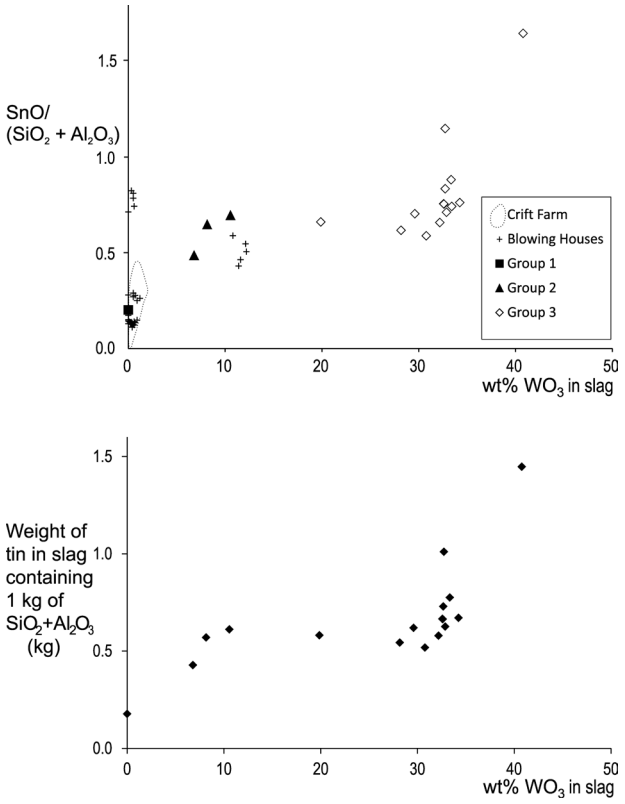

Figure 7: Upper: graph of $SnO/(SiO_2 + Al_2O_3)$ against WO_3. Analyses of slags from selected blowing houses and the field of analyses from slags from Crift Farm and are shown for comparison (data from Malham et al 2002). Lower: the Brownie Cross data rescaled to show the tin loss to the slag per unit weight of alumina plus silica in the slag.

of tin taken up by the slag, but for a slag of 40% WO_3 and containing the same amount of silica and alumina, as much as 1.6kg of tin will be taken up by the slag. Unfortunately, this cannot be used to determine the actual tin loss during smelting, for the wolframite content of the smelted ore remains unknown.

The slags with the higher contents of tungsten show the effects of increased viscosity, indicated by poor mixing and the preservation of emulsion textures. Although some areas of emulsion (see above) showed higher concentrations of tin prills in the more tungsten-rich zones, the low overall concentration of tin prills in the slags prevented demonstration of whether or not this was more generally true in the bulk slags.

Interpretation

The slag samples show several sets of features which allow some extraction of general properties. The overall morphology of the slag is difficult to interpret because of their highly fragmented state. However, a comparison of the external features and the internal structure does allow three forms to be recognised.

Samples AVN1, 2 and 5 have a rod-like form and are all dark glasses with a fibrous structure. AVN6 is a flap, possibly related. The rod-like, striated, fibrous rods are all from slag Groups 1 and 2. They resemble the most common slag morphology from Crift Farm. Although it might be possible to suggest that these derive from a different phase or process to the sheets, the relationship with the composition suggests that these silica rich (rather than tin-rich) glasses have been stretched during clearance because they are more plastic (slightly less viscous) than tin/tungsten-rich slags at the same temperature. The difference in texture may also suggest that they were separated from the tin in a slightly different way.

Samples AVN7, 13, 17, 19 and 20 have a sheet-form (Fig 8) and are typically 5-10mm thick. They commonly show a discrete basal layer, which may be vesicular, rich in tin and in particularly coarse crystals of tungstate A and may have tin-oxide dominated areas, occurrences of tungsten metal and crystals of hardhead. The basal facies of slag may also include minor amounts of very small crystals of olivine and spinel in some instances. The basal layer is abruptly overlain by a layer dominated by sub-vertical prismatic crystals of tungstate A in glass, which become finer upwards, trending towards dendritic growths in discrete domains. In some instances this zone preserves relict high-tungsten blebs, preserved in part by

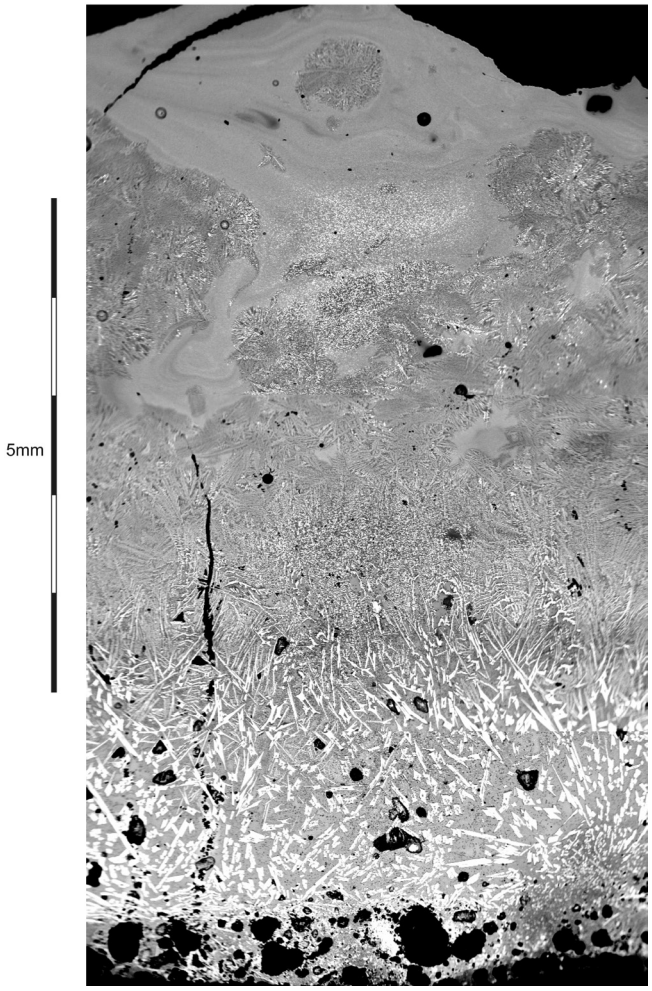

Figure 8: BSE micrograph montage of a section through an example of a typical slag sheet. The section shows the basal contact layer, with vesicles and abundant tin blebs and oxides, which has a rather abrupt contact with the overlying poorly-vesicular slag. Elongate large prisms of tungstate A grow off the boundary between the zones. The tungstate decreases in grainsize upwards into 'mossy' dendritic clumps, before passing into convoluted laminated glass. AVN7.

localised thickening of the tungstate prisms, indicating the slag flow was an emulsion. The uppermost development in the sheets is a fine-grained material, often appearing like glass in hand specimen, but under the SEM often seen to be at least partially microcrystalline (with crystallites probably of tungstate A). These finely crystalline zones may preserve a laminar texture, sometimes convoluted and sometimes an emulsion texture. In some instances, the sheets may contain coarse inclusions of derived materials including quartz, tungstate, tungsten, tin, and tin oxides. These fragments share many of the features of the more common inclusions or zone on the basal surface.

Samples AVN10, 12, 15 and 16 have a rounded, somewhat lobe-like form but with internal textures similar to those of the sheets. Although an origin as a flowed slag lobe is not impossible, it is considered more likely that these samples represent slag sheets deformed when partially solidified.

These features provide a series of close textural links between the majority of the tungsten-rich slags, whether from context 1146 or 1349B. The most easily identified set of characteristics is provided by the five slag sheet specimens. In general, it can be suggested that the slag was removed from the surface of the tin in a float (in early tin smelting, the metal was typically tapped from the furnace into a float, a basin usually carved into a large stone block, the floatstone, where the dross and slag separated from the metal by gravity, often assisted by poling with a green stick; after removal of the slag/dross the metal was ladled into a mould carved into another stone block, the mouldstone, to solidify). For the high silica glasses, this resulted in stringy, fibrous slag rods, but for the high-tungsten slags, the high liquidus and solidus temperatures, as well as the high viscosity, meant that the slags tended to deform less plastically – forming planar or twisted sheet fragments on removal.

The internal structures of the samples also display characteristics that appear repeatedly:

- inclusions with tin oxides, wolframite, tungsten, hardhead concentrated along the (assumed basal) margin of the slag sheet (AVN7, 10, 15 and 17) or dispersed within the body of the slag (AVN1, 19 and 20)
- laminar (hammerscale-like) inclusions (AVN5 and 17?)
- remnant emulsion textures (AVN10, 13, 16, 18 and 19).

The internal texture of the slag sheets suggests a highly viscous slag, in which mixtures of liquids of varying tin and tungsten contents failed to homogenise and the various materials separating from the tin became attached to the base of the slag, or were more rarely incorporated within it.

The scale-like material, with both iron and tin oxides, is suggestive of oxidation of the surface of the tin. Whether this was the result of a deliberate attempt to produce oxidising conditions to assist with the removal of iron from the tin, is not known but, perhaps, the relative scarcity of these particles may suggest that it was not.

Discussion

The implications of the Brownie Cross slags for medieval tin smelting are discussed in detail elsewhere (Taylor *et al* 2014). The site contains reasonable evidence for the

general location of features associated with the furnace, but these are very difficult to interpret. It is likely that the furnace itself was an above-ground stone construction, subsequently lost. It has been suggested that a stone-lined gully, adjacent to the likely furnace location, was a device to allow levelling of an overlying floatstone. A mouldstone was recovered from above a pit with similar packing just to the north and would have been capable of casting an ingot of up to 37kg. The evidence therefore suggests a manually-blown version of the typical late medieval blowing house.

Despite the small size of the slag fragments from the site, there is no evidence that this is due to the reprocessing of slag. Rather, it is believed that the small fragments result from the scraping of a thin layer of partially solidified slag from the surface of the tin in the float.

Unlike the slags so far described from Crift Farm, Cornwall (Malham *et al* 2002; dated on the basis of an associated iron-working hearth to a period between the 9th and 13th centuries, cal AD 896-1210; OxA-2400), the Brownie Cross slags contained persistent, if rare, inclusions of oxidised tin, tungsten metal and hardhead. Some of the inclusions were probably swept out of the furnace with the slag flow, but most are segregated in the basal layer of the slag and may have separated from the molten tin in the float. There is no evidence, however, that this indicates a problem with tin quality; all the analysed tin prills were of high purity. Rather, it indicates an efficient use of the float. The precise mode of formation of the lower layer of the slag remains uncertain. Many of the components (including hardhead, tungsten and wolframite) are denser than liquid tin and it may be that they have been collected from the tin by the formation of the lower-density tin oxides which contain them, perhaps by poling.

There is no evidence that the slags at Brownie Cross represent more than one process. Their composition and textures show a continuum, with many shared features between samples and with the variation between them linked to compositional changes that are unlikely to be indicative of a staged process (*ie* they are all most likely to represent a simple, single-stage smelting process). The chemical differences between the groups of slags examined here may be explained through the exploitation of slightly different ores. Group 1 material, represented by a single slag sample, is compositionally similar to slag from Crift Farm and can be interpreted as waste from the smelting of an ore batch uncontaminated by wolframite. Group 3 slags are particularly rich in tungsten and must indicate smelting of cassiterite strongly contaminated by wolframite. The Group 2 slags are characterised by intermediate tungsten levels, and also by being relatively more aluminium- and titanium-rich, features which suggest incorporation of mineral grains derived from titanium-rich haematite veins, which occur in various locations within the Dartmoor granite. This variation in slag chemistry may reflect the derivation of alluvial ores from various places within the Tory Brook or Wotter Brook valleys, which run down from Dartmoor between Brownie Cross and Hemerdon Ball.

The compositional slag groups show some stratigraphic control; the earlier of the two sampled contexts (1349; assigned to phase Working (i)) provided all the samples in compositional Groups 1 and 2, and just 3 of 13 from Group 3, whereas the later context (1146; assigned to phase Working (ii)) provided the remaining 10 Group 3 samples. The samples from context 1146 also include all five of the examples of evidence for an emulsion of two liquids and four of the five examples of the association of tungsten-hardhead-tin-coarse tungstate A. The sources being worked when the fills of 1146 were deposited were therefore, on average, slightly more tungsten-rich and slightly less titanium-rich than those being worked when the slags in 1349 were generated.

The occurrence of metallic tungsten in the Brownie Cross slags predates the discovery of metallic tungsten by 500 years. There are several previous records of early metallic tungsten from SW England. The most extraordinary of these is the Trewhiddle bloom (Rehren 2005). This object resembles an iron bloom, but comprises metallic tin, containing inclusions of hardhead, intermixed with sub-spherical particles of tungsten embedded in a matrix of an iron-tungsten alloy. The tungsten particles are approximately 10µm in diameter, rather larger than the sub-spherical components of the aggregate in AVN1 (typically up to about 5µm) and much larger than the more isolated rounded particles in AVN10 and AVN20, but of broadly similar size to the tungsten particles overgrown by tungstate A in AVN17. The origin of the bloom itself is uncertain – it is undated and it remains unclear if it is from an early experiment with tungsten or if it is simply a fortuitous by-product from a smelt intended to produce either tin or iron. Small quantities of metallic tungsten have also been described by Malham (2010) in her unpublished thesis: she illustrated tungsten in a tin prill from High Down (fig A13.5) and describes (p.307) prills of tungsten in reverberatory furnace slags from Carvedras. Further examples of tungsten in reverberatory furnace slags have been described, also in an unpublished thesis, by Farthing (2002).

Of the five occurrences of tungsten metal in the Brownie Cross samples (AVN1, 10, 17, 19 and 20), four (and possibly all five) are associated with tin (or oxidised tin), two with hardhead, and four with an overgrowth of tungstate A. In three of the five cases the samples also contain unusually coarse-grained tungstate A (either directly or indirectly associated with the tungsten). These features suggest that there is a link between these occurrences, with all reflecting incorporation of particulate materials from high-temperature growth.

The chemical trends within the tungsten-rich slags have demonstrated the significance of the term 'wolf's foam' for a tungsten-rich tin smelting slag devouring tin. The viscous nature of the slag, as indicated by the flow foliation and the preservation of emulsion textures, led to the trapping of tin prills – and particularly so once the network of crystals of the tungstate A had started to form. However, this is only part of the story, for the glass phase of the tungsten-rich examples also has an enhanced content of tin, apparently as a network-forming element. The combined effect of these features would have led to significant tin-loss. The identification of emulsions within the molten slag is interesting, and raises the question of whether this effect would have been visible and contributed towards the choice of the old German expression.

SW Dartmoor became a more significant area of production in the later medieval period, culminating in the elevation of Plympton to a Stannary Town in 1328 (argued by Taylor *et al* (2014, 264) to have occurred shortly after the period of operation of the Brownie Cross smelter). The continuation of the Brownie Cross operation despite the problems with tungsten, which would have significantly reduced the yield, reflects the high value of tin in the medieval period.

Appendix: slag mineralogy

Spinels: three groups of spinels were identified in Group 2 slags – a close to end-member magnetite (ideally Fe_3O_4), a phase with a composition corresponding to a heavily Ti- and Al-substituted magnetite and a hercynite (ideally $FeAl_2O_4$) with major magnesium substitution. The 'Ti- and Al-substituted magnetite' shows approximately 0.5 atoms of titanium, 0.7 atoms of aluminium, 0.07 atoms of magnesium, 0.1 atoms of magnesium and 1.6 atoms of iron per formula unit (calculated with 4 oxygens). This does not appear to be a true mineral composition and is likely to be a mixture of titanium-rich and aluminium-rich phases. In AVN2 this material lies at the core of zoned spinels, the outer parts of which are of Mg-hercynite (see below) and may thus be a mixture of a titanium-rich mineral (ulvite?; ideally Fe_2TiO_4) and Mg-hercynite.

The hercynite shows minor substitution of manganese and major substitution of magnesium for iron, corresponding to a range of 18-51% of the spinel (*sensu stricto*; ideally $MgAl_2O_4$)) end member. In AVN2 this material forms the outer part of zoned euhedral spinel grains with Ti-rich cores. In this context the degree of Mg replacement rises slightly from inner to marginal parts of the grain. In AVN2 poorly-delimited Mg-hercynite also appears to locally overgrow ilmenite.

Ilmenite: Ilmenite ($FeTiO_3$) was present in the Group 2 slag, AVN2, as narrow (2-4μm wide), elongate, segmented to dendritic crystals. It formed later than the spinels, the cordierite and the possible rhönite.

Ti-bearing alumino-silicate: the Group 2 slag, AVN2, contained a finely dendritic mineral of low-electron density, which was closely associated with the ilmenite in the sample. Identification of this material was not possible because of its fine grain size and rather diffuse appearance even at high magnification. The best analyses of the phase suggest a composition close to that of a rhönite-aenigmatite group mineral, but the identification is not certain and the morphology does not resemble the usual morphology of rhönite in slags (both rhönite (ideally $Ca_4(Mg_8Fe_2^{3+}Ti_2)O_4[Si_6Al_6O_{36}]$) and aenigmatite (ideally $Na_4(Fe_{10}^{2+}Ti_2)O_4[Si_{12}O_{36}]$) were, however, reported in tin slags by Chirikure *et al* 2010). The analyses show appreciable levels of both sodium and potassium.

Cordierite ($Mg_2Al_3(AlSi_5)O_{18}$): this phase was only identified in a limited area of the Group 2 slag, AVN2, in which it appears as hexagonal-sectioned euhedral grains 5-10μm across.

Scheelite (ideally $CaWO_4$): this phase was identified only in the Group 2 slag, AVN2, in which it occurs as stubby, angular, dendrites. The analyses show low levels of iron and tin, with a slight deficiency of calcium compared to tungsten. It is likely that some of these impurities are present as phase inclusions rather than as impurities in the scheelite itself. The morphology indicates that this scheelite is neoform and not inherited from the furnace feed.

Wolframite group: the slags contained various textural components of wolframite group minerals (Fig 9). Wolframite itself refers to minerals with compositions

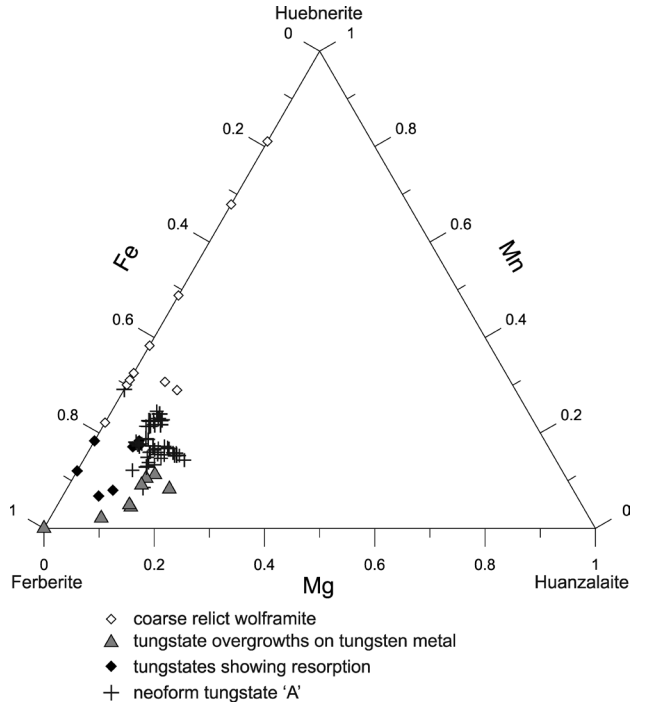

Figure 9: EDS analyses of wolframite group minerals. Natural wolframite lies between ferberite ($FeWO_4$) and hueberite ($MnWO_4$). The magnesium end-member of the wolframite group (MgWO4; huanzalaite) has not been observed in solid solution with wolframite in nature.

between the iron end-member (ferberite, $FeWO_4$) and the manganese end-member (hueberite, $MnWO_4$). The broader wolframite group also contains zinc and magnesium end-members which show little natural solid solution with wolframite *sensu stricto*.

Coarse grains of wolframite occurred sporadically, particularly near the base of slag sheets (see below) and are interpreted as relict grains, sometimes showing carious textures and rounded indented outlines (Fig 6a), suggesting they had undergone some resorption. Almost all the grains identified as probably being relict on textural criteria produced analyses lying on the ferberite-huebnerite join (ranging from 19%-78% ferberite), compatible with being natural mineral grains.

The major crystalline component of the tungsten-rich Group 3 slags is a phase for which there appears to be no equivalent in the published literature. It typically occurred as elongate neoform crystals (*ie* they have crystallised from the slag melt, rather than being relict as with the wolframite described above), often approximately square in cross-section and frequently hollow (Fig 3c). XRD suggests it is a wolframite group mineral, in which case the EDS analyses can be expressed as 67-78% (average 71%) of ferberite, 12-25% (average 17%) of huebnerite and 8-19% (average 12%) of huanzalaite (the magnesium end-member of the wolframite group, $MgWO_4$). Huanzalaite is a rare mineral, discovered only recently as inclusions within scheelite (Miyawaki *et al* 2010), but which has not been observed in significant solid solution within natural wolframite of the ferberite-huebnerite group. Neither the scheelite not wolframite groups are known to allow magnesium to substitute for iron in nature – in the case of Chang's (1967) study of scheelite, solid solution of magnesium was limited to below 2%. There is a degree of solid solution between the wolframite and scheelite ($CaWO_4$) groups at high temperature (Grubb 1967) leading to exsolution on cooling. Until this crystalline component of the Group 3 slags is fully understood it is referred to as tungstate A, for it is possible that it is a low-magnesium wolframite with fine-scale huanzalaite inclusions, rather than a mineral of the wolframite group with a previously-undocumented degree of magnesium subsitution. This phase occurred in all samples of the group.

Where particles of tungsten metal occurred, they showed overgrowth by tungstates, with a range of apparent compositions from end-member ferberite, through to compositions with up to 19% huanzalaite and up to 11% huebnerite. The most substituted compositions were somewhat manganese-poor compared with typical tungstate A.

A small proportion of the coarse grains that show probable resorption were not natural wolframite, but were tungstate A (see below); they had a range of compositions with 74-88% ferberite and up to 9% huanzalaite. Presumably these were early-formed within the smelting furnace (Fig 6b).

Olivine: olivine group minerals ($(Fe,Mg,Mn,Ca)SiO_4$) were recorded as a minor component from three samples in Groups 2 and 3 (AVN5, 7 and 17). In AVN5 the olivine crystals were growing off the 'scale'-like oxide sheet, whereas in AVN7 and AVN17 they were close to coarse-grained tungstate A. The olivine was compositionally different in the three examples, but was consistent within each example. In AVN5 the olivines were $Fa_{70\text{-}72}Fo_{30\text{-}28}$ with 2% manganese substitution (olivine composition is here expressed as a composition on the fayalite (Fa) - forsterite (Fo) solid solution, with manganese substitution expressed as a percentage). In AVN7 they were $Fa_{85\text{-}87}Fo_{15\text{-}13}$ with 7-8% manganese substation. Those in AVN17 were more magnesian at $Fa_{56\text{-}57}Fo_{44\text{-}43}$ with 6-7% manganese substitution.

Tin: prills of tin occur widely in the slags and were observed in all samples. They are very small (mainly

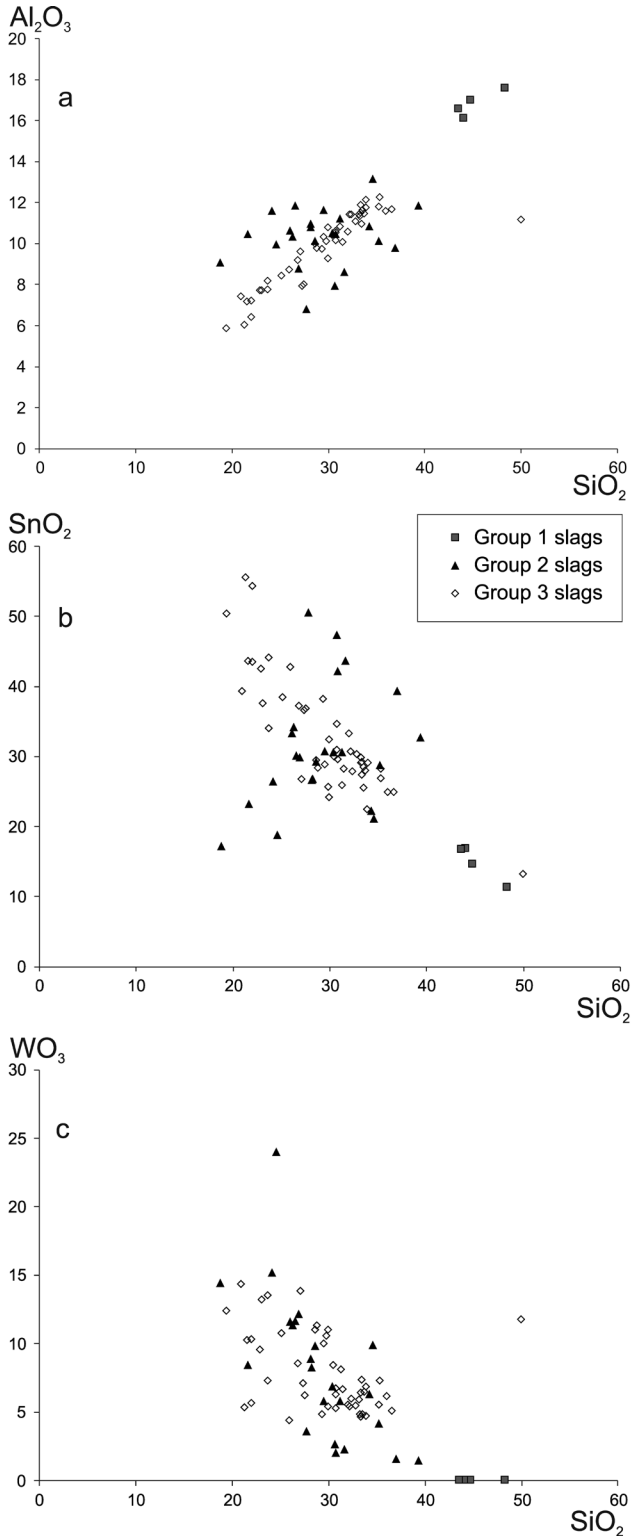

Figure 10: Plots showing aspects of the chemical composition of the glass phase. Analyses are of individual areas by EDS.

<10µm, almost all <50µm, but rare examples were up to 500µm). Wherever analysed, the tin appeared to be of high purity, although frequently oxidised. Iron was occasionally recorded at close to the limit of detection. The available evidence therefore suggests the production of good quality of tin, although the small prills are not necessarily representative of the bulk metal produced.

Glass: the glass phase (or what has been assumed to be glass – it may be microcrystalline in some cases) is only moderately siliceous in the Group 1 slag, at 43-48% SiO_2 (Fig 10a), around 17% Al_2O_3 (*ie* SiO_2:Al_2O_3 = 2.7), with moderate levels of iron (11% expressed as FeO) and TiO_2 (3.6%), but with a fairly high tin content (average 16% SnO_2). Glass in slags of Groups 2 and 3 has a variable composition, with parallel trends of enrichment in SnO_2 and WO_3 (Fig 10b and 10c). The glass of .Group 2 slags also shows a very variable SiO_2:Al_2O_3 ratio.

The observation of the enrichment of the glass phase in both tungsten and tin is important, for it demonstrates that the trapping of tin metal prills by the network of tungstate 'A' crystals is not the only mechanism for the loss of tin to high-tungsten slags.

High-tin glasses have been discussed by Chirikure *et al* (2010, 1663-4). They observed an inverse correlation between tin oxide and silica in the glasses of slags from Rooiberg, indicating that under reducing conditions SnO becomes a network-former in the glass. Both SnO and WO_3 will act to increase the viscosity of the glass, whereas FeO will tend to reduce it. The ratio of FeO:(SnO+WO_3) will thus be an indicator of viscosity: a high ratio will give a low viscosity, a tendency for crystallisation and easier slag-metal separation; the converse will be true for examples with a low ratio, leading to increased tin losses in smelting.

References

Alderton D H M, 1993, 'Mineralization associated with the Cornubian granite batholith', in R A D Pattrick and D Polya (eds), *Mineralization in the British Isles* (London), 270–354.

Bandy M C and Bandy J A (tr) 1955, *De natura fossilium*, Translated from the first Latin edition of 1546 (New York: Geological Society of America Special Paper 63).

Bray C and Spooner E T C 1983, 'Sheeted vein Sn-W mineralization and greisenization associated with economic kaolinization, Goonbarrow china clay pit, St. Austell, Cornwall, England; geologic relationships and geochronology', *Economic Geology* 78, 1064-1089.

Chang L L Y 1967, 'Solid solutions of scheelite with other $R^{II}WO_4$-type tungstates', *American Mineralogist* 52, 427-435.

Chirikure S, Heimann R B and Killick D 2010, 'The technology of tin smelting in the Rooiberg Valley, Limpopo Province, South Africa, ca. 1650-1850 CE', *Journal of Archaeological Science* 37, 1656-1669.

Dines H G 1956, *The metalliferous mining region of south-west England*, (London).

Dunkle S E, Craig J R, Rimstidt J D and Lusardi W R 2003, 'Romarchite, hydroromarchite and abhurite formed during the corrosion of pewter artifacts from the Queen Anne's Revenge (1718)', *Canadian Mineralogist* 41, 659-669.

Farthing D 2002, The mineralogy of tin slags, unpublished PhD thesis, Johns Hopkins University, Baltimore.

Grubb P L C 1967, 'Solid solution relationships between wolframite and scheelite', *American Mineralogist* 52, 418-426.
Henckel J 1725, *Pyritologia oder Kiess-Historie* (Leipzig).
Louis H 1911, *The metallurgy of tin* (New York).
Luyart J and Luyart F 1783, 'Analisis quimico del volfram, y examen de un nuevo metal, que entra en su composition', *Extractos de las Juntas Generales Celebradas por la Real Sociedad Bascongada de los Amigos del Pais en la Ciudad de Vitoria pro Setiembre de 1783*, 46-88.
Malham A 2010, The classification and interpretation of tin smelting remains from south west England: A study of the microstructure and chemical composition of tin smelting slags from Devon and Cornwall, and the effect of technological developments upon the character of slags, unpublished PhD thesis, University of Bradford.
Malham A, Aylett J, Higgs E and McDonnell J G 2002, 'Tin smelting slags from Crift Farm, Cornwall, and the effect of changing technology on slag composition', *Historical Metallurgy* 36, 84-94.
Miyawaki R, Yokoyama K, Matsubara S, Furuta H, Gomi A, Murakami R 2010, 'Huanzalaite, $MgWO_4$, a new mineral species from the Huanzala mine, Peru', *Canadian Mineralogist* 48, 105-112.
Pryce W 1778, *Mineralogia cornubiensis: a treatise on minerals, mines, and mining* (London).
Rehren T 2005 'The Trewhiddle tungsten bloom', *ITIA Newsletter* June 2005, 2-5.
Scheele C W 1781, 'Tungstens beståndS-delar', *Kongliga Vetenskaps Academiens Nya Handlingar* 2, 89-95.
Sisco A G and Smith C S (tr) 1951, *Lazarus Ercker's treatise on ores and assaying*, (Chicago).
Taylor S R, Jones A M and Young T 2014, 'Smelting point: archaeological investigations along the route of the Avon Water Main Renewal, Plympton, Devon 2009', *Proceedings of the Devon Archaeological Society* 72, 187-276.
Wallerius J G 1747, *Mineralogia, eller Mineralriket* (Stockholm).
Young T P 2011, Archaeometallurgical residues from field D1, Brownie Cross, Shaugh Prior, Devon (Avon SWW Pipeline) (GeoArch Report 2011/43).
Young T P and Kearns T 2011, Evaluation of archaeometallurgical residues from sites D1 and D5, Avon SWW pipeline, Devon (GeoArch Report 2010/08).

The authors

Tim Young runs the GeoArch consultancy, providing a service in archaeometallurgical analysis, as well as other aspects of archaeological science. His personal research interests are mainly in ferrous archaeometallurgy of all periods.
Address: GeoArch, Unit 6 Block C, Western Industrial Estate, Caerphilly CF83 1BQ.
Email: Tim.Young@GeoArch.co.uk

Sean Taylor works for the Cornwall Archaeological Unit as an Archaeology Project Officer, managing and directing mainly developer-funded projects.
Address: Cornwall Archaeological Unit, Cornwall Council, Fal Building, County Hall, Treyew Road, Truro TR1 3AY.
Email: setaylor@cornwall.gov.uk